STRESS AND FATIGUE ANALYSIS OF DRIVING WHEEL TOOTH BASED ON ORTHOGONAL DESIGN

Hefeng ZHANG, Bijuan YAN[1], Tiangang PEI, Zhangda ZHAO*

To address the problem of excessive tooth root strength of the driving wheel during walking of a heavy spreader, this paper uses orthogonal design method to optimize the sprocket tooth structure parameters. The rigid-flexible coupling model of track mechanism is established based on dynamics software Recurdyn. The model is simulated under typical working conditions, and the stress and fatigue life of sprocket teeth is obtained. Then the orthogonal table with different tooth parameter size combinations is established based on orthogonal principle. And the orthogonal combination results are obtained by dynamics simulation and analyzed by variance and range method. Comparing the tooth strength before and after orthogonal optimization, it is found that stress of the tooth root is reduced by 7.5 %, fatigue life is increased by 8.9 %, which improves the service life of the driving wheel. The research results provide reference for the design of other structural parameter.

Keywords: Sprocket, dynamics simulation, variance analysis, range analysis

1. Introduction

Crawler travel mechanism is an important walking structure of a heavy spreader. The sprocket is a significant part of crawler walking mechanism. Its teeth are subjected to excessive loads during the use of the sprocket, resulting in a shortened fatigue life of the sprocket, which causes a series of additional consumption such as the running cost of the sprocket and maintenance time, maintenance costs, etc., and seriously affects service life of crawler travel mechanism and overall effectiveness of entire spreader. Therefore, it is essential to reduce stress of sprocket teeth.

In order to solve the above problems, some scholars optimize the gear tooth surface. For example, Ding et al. [1] proposed a tooth surface shaping method to

[1] Prof.,College of Mechanical Engineering, Taiyuan University of Science and Technology, China, e-mail:2006084@tyust.edu.cn

* Corresponding author: zzd@stu.tyust.edu.cn

find the optimum amount of corner shaping, to increase the service life. Wang et al. [2] proposed a multi-objective optimization method to optimize the helical gear from the perspective of tooth profile modification. Ren et al. [3] proposed a method of cycloidal gear trimming to improve the load -carrying capacity of cycloid gears by adjusting the positions of five key points on the gear teeth to determine a corrected clearance curve. Yan et al. [4] used a dynamic tooth width correction method to optimize the uneven loading problem of helical gears. And Wang et al. [5] proposed a calculation method for tooth profile modification based on the tooth contact analysis (TCA) technique.

The methods used in the above citation are based on modifying the tooth surface shape to improve the tooth strength. But it is not difficult to analyze the influence of the gear tooth size on the tooth root stress. Orthogonal experimental design is a method for investigating the effect of multiple factors and levels on the test index. In order to saw the optimal combination of factors for the test index, Yin et al. [6] optimized the key structural parameters of the dust collector based on the principle of orthogonal experiments so as to improve the efficiency of the dust removal system. Kuang et al. [7] optimize the key structural parameters of the drilling tool using the orthogonal optimization method, so as to improve the bending strength of the drilling tool joint in the actual working process. Liu et al. [8] analyzed the influence of spraying parameters on coating properties by orthogonal test method, and found that the optimized coating has better wear resistance through experimental comparison.

In this paper, based on the principle of orthogonal experiments, a three-factor and three-level orthogonal table is established, and a rigid-flexible coupling track model with different sizes of sprocket teeth as the flexible body is built based on the parameter combination of the teeth in the orthogonal table. The optimized sprocket teeth were simulated using dynamics software to obtain the stress and fatigue clouds of the sprocket teeth under different working conditions. Compared with stress and fatigue clouds of sprocket teeth before optimization, it was found that the strength of optimized sprocket teeth was improved. This provides a theoretical reference for the mechanical design of the crawler travel mechanism.

2. Modeling and Simulation of Crawler Walking Mechanism

2.1. Creation of the Model

Fig. 1 shows completed three-dimensional (3D) crawler travel mechanism model. The 3D modeling of the studied spreader is carried out based on the product

manual and technical drawings of a certain type of spreader. A spreader is mainly composed of a crawler travel mechanism, discharge arm, balance beam, receiving arm, and other components. If all parts are imported, it will take up a lot of computer resources, seriously affect the simulation speed and the simulation is error-prone, so it is necessary to simplify the spreader model. The stress analysis of the sprocket tooth is mainly carried out. Therefore, in the modeling, the equivalent mass and equivalent moment of a inertia ball are used to replace the components that have little influence on crawler travel mechanism [9, 10]. The 3D model of crawler travel mechanism is established by software SolidWorks and imported into dynamics software RecurDyn in the form of an x_t file.

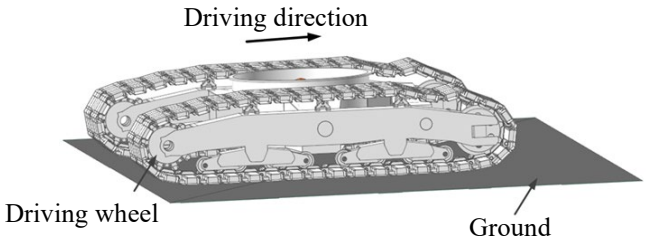

Fig.1. 3D model of crawler travel mechanism

The stress analysis of sprocket teeth is carried out. Firstly, the key parameters of a crawler travel mechanism are described. The weight of the spreader is 6.5e5 kg , the walking speed is 8 m/min, the diameter of the sprocket pitch is 1.674 m, the track grounding length is 9.814 m, and the track gauge is 10 m. The main parameters of the sprocket are shown in Table 1.

Table 1

Related parameters of sprocket

Name	Value	Name	Value
Number of teeth (z)	9	Tooth depth (mm)	134
Pitch diameter of sprocket (mm)	1674	Tooth root thickness (mm)	57
Tooth thickness (mm)	161	Root diameter (mm)	50

Figure 2 shows sprocket structure. It mainly includes hub and tooth, in which are connected by bolts. During walking process of crawler travel mechanism, force analysis of meshing process between sprocket and track shoes is carried out. The tooth root of sprocket is determined as main bearing position. Tooth thickness, tooth depth, and tooth root thickness are three key parameters of the sprocket [11-14].

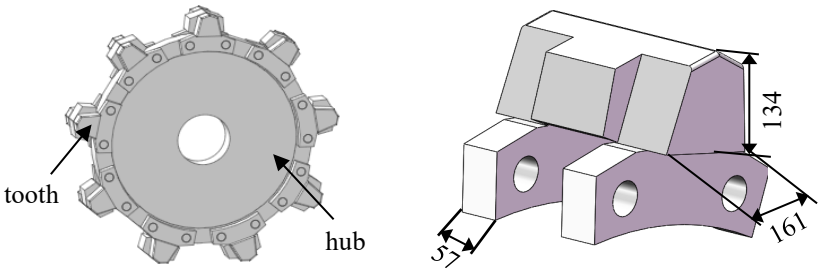

i) Sprocket model ii) Sprocket tooth parameter model

Fig.2. 3D model of sprocket

2.2. Boundary Condition Setting

In ANSYS Workbench, the sprocket tooth material is set as 23MnCrNiMo, the Poisson's ratio is 0.25, and the elastic modulus is 210 GPa. When the driving wheel is stressed, it is equivalent to the cantilever beam. The rigid-flexible coupling model takes a long time to simulate. In order to reduce the simulation time, only the mesh of the tooth of the sprocket is divided and the mesh of the tooth root is refined. The overall mesh size of sprocket tooth is 25 mm, and the mesh size of its root is 20 mm. In the dynamic software RecurDyn, The sprocket tooth in the original rigid track travel meshed to complete the establishment of the sprocket tooth's flexible body. The rigid-flexible coupling model of the sprocket with tooth as flexible body is established [10, 15-18].

The friction contact is created between the flexible sprocket tooth and the track shoes. The dynamic friction coefficient is set to 0.15, and the static friction coefficient is set to 0.2. Force Distributing Rigid (FDR) is created between the wheel hub and sprocket teeth to realize force transmission. The driving speed is applied to the sprocket, and its function expression is STEP (time, 0.1, 0, 1, 0.1593). The function is a step function, which means that when the simulation time is 0-0.1s, the driving wheel rotation speed is 0 rad/s. When the simulation time is 0.1 s -1 s, the driving wheel is in the acceleration stage, and its rotation speed increases from 0 rad/s to 0.1593 rad/s. Then its rotation speed remains 0.1593 rad/s after 1 s. The dynamic simulation of the rigid-flexible coupling model of crawler travel mechanism is carried out to obtain the stress and fatigue life distribution of the sprocket tooth.

2.3. Model Simulation and Analysis

According to the actual running situation of spreader, simulation typical working conditions of flat road straight, uphill straight and In-situ steering are

determined. The model of track walking mechanism was simulated. The driving torque of driving wheel under different working conditions is obtained, which are shown in Figure 3. The average driving torque of the driving wheel under different working conditions can be obtained from Figure 3, as shown in Table 2.

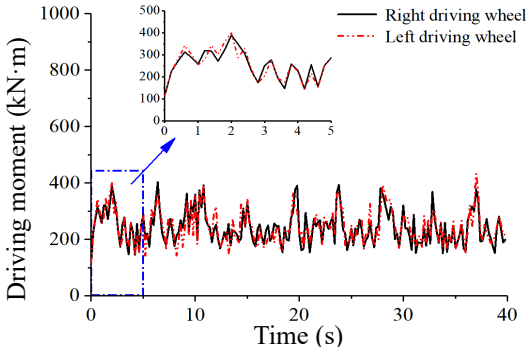

i) Straight road conditions

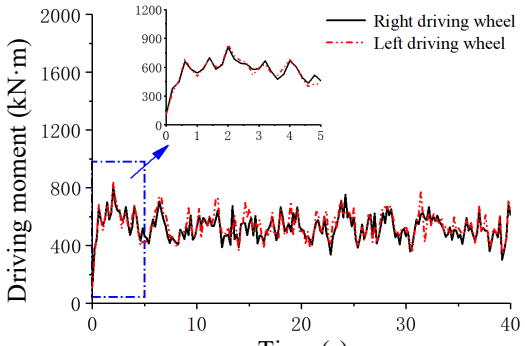

ii) Hill climbing conditions

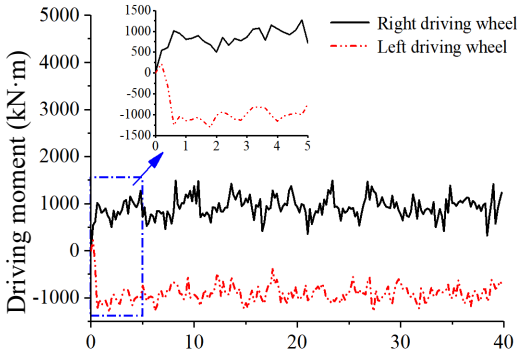

iii) In-situ steering conditions

Fig.3 Driving torque of driving wheel under different working conditions

Driving wheel driving torque is calculated by theoretical calculation under typical working conditions. The driving torque under different working conditions is obtained, as shown in Table 2.

Under three working conditions, the simulation and theoretical values of the driving wheel are within 10 %, as shown in Table 2, indicating the correctness of the model parameter Settings.

Table2

Comparison of theoretical and simulation values of driving torque under different working conditions

	Straight road	Hill climbing	In-situ steering
Simulation value (kN·m)	260	550	980
Theoretical value (kN·m)	272	541	939
Rate (%)	4.4	1.6	4.3

Using dynamics software RecurDyn, the rigid-flexible coupling model of crawler travel mechanism is simulated. And then based on the rigid-flexible coupling simulation results, the fatigue life of a tooth of the sprocket is calculated by using the dynamic stress recovery method. The stress and fatigue distributions on sprocket teeth under different working conditions are obtained, which are shown in Figure 4. Code 39 in Figure 4 is the maximum stress node on one tooth of driving wheel in the walking process of crawler walking mechanism.

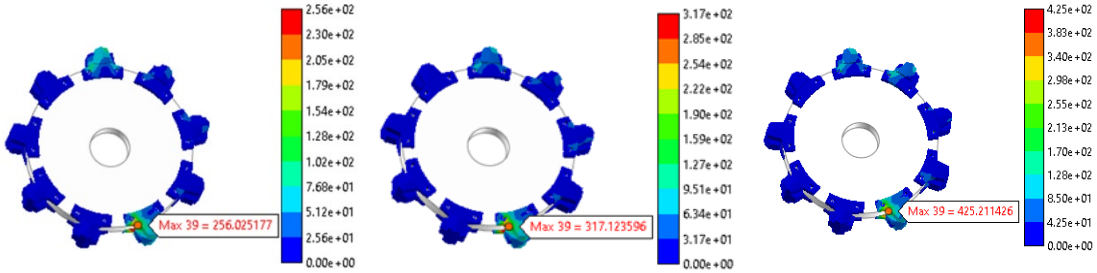

i) Straight road conditions ii) Hill climbing conditions iii) In-situ steering conditions

a) Sprocket teeth stress nephogram (MPa)

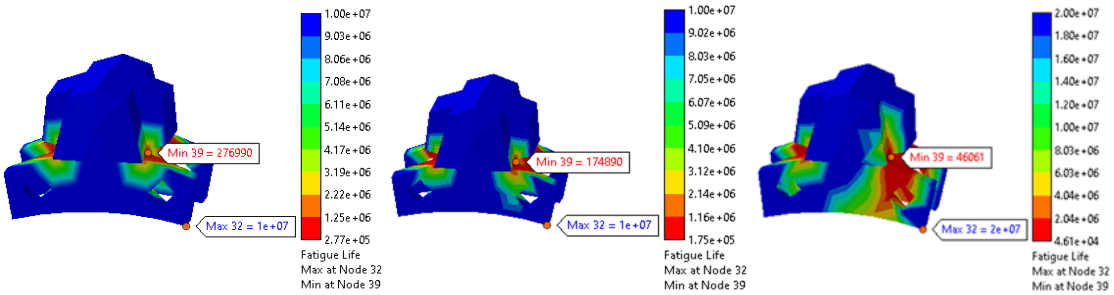

i) Straight road conditions ii) Hill climbing conditions iii) In-situ steering conditions

b) Sprocket tooth fatigue nephogram

Fig.4. Sprocket tooth stress and fatigue nephogram

It can be seen from Figure 4 a) that maximum stress of code 39 on sprocket teeth of crawler traveling mechanism is 256 MPa under straight road condition. Its maximum stress of code 39 is 317 MPa under the hill climbing condition. The maximum stress of code 39 is 425 MPa under in-situ steering condition. It can be seen from Figure 4 b) that minimum fatigue times on sprocket teeth are 276990 under straight road condition. The minimum fatigue times are 174890 when climbing straight. Under in-situ steering, the minimum fatigue times is 46061. Therefore, the stress at the tooth root of sprocket is the maximum, and the fatigue life is the smallest during walking process of crawler travel mechanism. The maximum stress of sprocket tooth increases in turn and its fatigue life decreases in turn under the three working conditions of straight road, hill climbing, and in-situ steering. Based on strength analysis of sprocket teeth under different working conditions, the root of sprocket teeth is the weakest part of the whole tooth, and the weak area is modified accordingly, to improve the service life of the part.

3. Orthogonal Optimization

3.1. Orthogonal Array

In order to facilitate the expression, symbol A is used to represent the tooth thickness parameter, B is the tooth depth, and C is the tooth root thickness parameter. In order to reduce number of orthogonal combination tests, three levels are selected for each factor among three key factors of sprocket teeth. Change of factor A is 5 mm, that of factor B is 5 mm, and that of factor C is 3 mm. Then, A is taken as 156 mm, 161 mm and 166 mm, B is taken as 129 mm, 134 mm and 139 mm, and C is taken as 54 mm, 57 mm and 60 mm. The orthogonal sequence design combination

of A, B, and C are obtained, shown in Table 3. It represents corresponding sprocket parameter size combination. According to nine groups of orthogonal size combinations, the rigid-flexible coupling models of crawler travel mechanism with different sizes of sprocket teeth as flexible bodies are established [19-21], and the dynamic simulation of the model is carried out. The results of different experiment sequence combinations are shown in Table 3.

Table 3

Results of orthogonal experiment

Experiment No.	A	B	C	Simulation result (MPa)
1	1	1	1	359
2	1	2	2	245
3	1	3	3	236
4	2	1	2	338
5	2	2	3	233
6	2	3	1	288
7	3	1	3	293
8	3	2	1	245
9	3	3	2	259

3.2. Analysis of Range

In order to analyze the influence weight of each factor on sprocket tooth strength, and find the main factors affecting the effect and the optimization scheme, the range analysis of simulation results is needed. The analysis results are shown in Table 4. In the table, k_i is the sum of several simulation indexes at corresponding level i, M_i is the average value of the index at corresponding level i, and R is the range of each average value. The range indicates weight of level selected under each factor on test index. The greater the range indicates the greater the weight of level change of the factor on test index [22-23].

Table 4

Range analysis of each factor on tooth root stress

--	A	B	C
K_1	840	990	892
K_2	859	723	842
K_3	797	783	762
M_1	280	330	297.3
M_2	286.3	241	280.7

M_3	265.7	261	254
R	25.7	89	43.3

In order to more intuitively reflect the influence of horizontal change of factors on test results, horizontal change of factors is taken as the abscissa and average value of the index is taken as the ordinate. The diagram of relationship between factors and the index is shown in Figure 5.

The magnitude of the difference of each factor reflects the influence of tooth thickness, tooth depth, and tooth root thickness on sprocket tooth stress. Figure 5 shows that the influence of each factor on sprocket tooth stress is different. Range of factors A, B, and C are 20.7, 89, and 43.3, respectively. Therefore, it is known that the order of the influence of the selected size parameters on the stress is B > C > A.

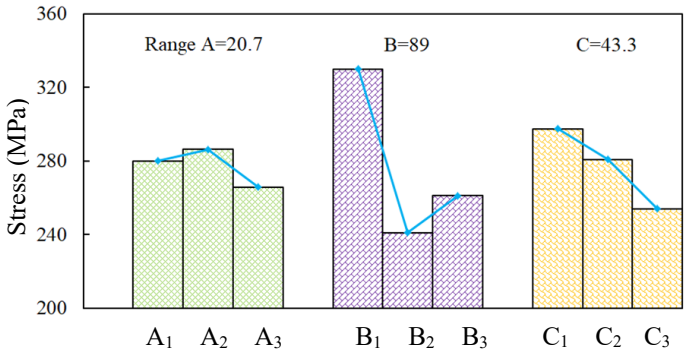

Fig.5. Relationship between factors and indicator

For a single factor, comparing the values of experiment index under each level of a factor, the order of the influence of each level of the factor on the index can be obtained. It can be seen from Figure 5 that the tooth root stress increases first and then decreases with the increase of factor A, and the order of the influence of each level of factor A on the tooth root stress is A_2, A_1, and A_3. The tooth root stress decreases with the increase of factor C, and the decrease rate is first small and then large. The influence of factor C on tooth root stress is in the order of C_1, C_2, and C_3. The tooth root stress decreases first and then increases with the increase of factor B. Therefore, the tooth root stress can be obtained by taking intermediate value of factor B at the horizontal level.

Given what the intermediate value of factor B is worth to obtain the minimum stress of the sprocket tooth, in this case, two points are taken on both sides of the intermediate value B_2 at the level of factor B, and these two points are respectively at the midpoint between B_1 and B_2 and between B_2 and B_3. A new three-

factor three-level orthogonal experiment is composed of the obtained two points and the original intermediate value B_2. According to the new orthogonal experimental group, a rigid-flexible model is established, and its dynamic simulation is carried out. The range analysis of obtained orthogonal results is carried out, and the obtained range and the original range are marked in Figure 6. The relationship between factor B and the stress is fitted by quadratic function fitting method, as shown in Figure 6.

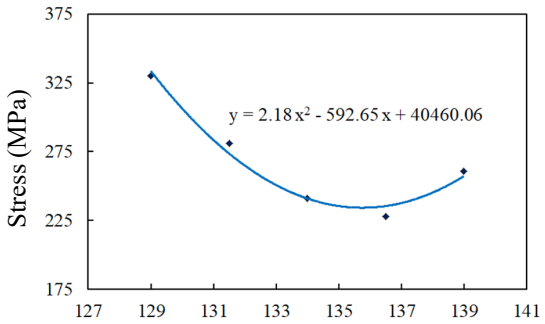

Fig.6. Factor B fitting curve

It can be seen from Figure 6 that according to the results of the quadratic fitting curve, the optimal factor B level value and the minimum stress value of sprocket tooth can be obtained by taking the vertex coordinates of the fitting curve, and the optimal value of factor B is 136 mm.

To sum up, according to the line chart and curve-fitting results, the optimal combination of selected parameters can be obtained. The value of factor A is 166 mm, factor B is 136 mm and factor C is 60 mm. This is the optimal structural parameter value of the sprocket teeth and its optimal combination within orthogonal optimization range.

3.3. Mathematical Model of Variance Analysis

Orthogonal experimental index is tooth root stress (von Mises), expressed by σ . Without considering interaction of various factors. The sum of deviation squares of factors A, B and C were represented by S_A, S_B, and S_C respectively, which is determined using Eqs.(1)-(3). Then, the sum of error squares is represented by S_e, which is determined using Eqs.(4).

$$S_A = \frac{1}{h}\sum_{j=1}^{h} M_{Ai}^2 - \frac{1}{n}\sum_{ii=1}^{n} k_{ii} \tag{1}$$

$$S_B = \frac{1}{h}\sum_{i=1}^{h} M_{Bi}^2 - \frac{1}{n}\sum_{ii=1}^{n} k_{ii} \tag{2}$$

$$S_C = \frac{1}{h}\sum_{i=1}^{h} M_{Ci}^2 - \frac{1}{n}\sum_{ii=1}^{n} k_{ii} \tag{3}$$

$$S_e = \frac{n+2}{n}\sum_{ii=1}^{n}(k_{ii}^2 + k_{ii}) - \frac{1}{h}\sum_{i=1}^{h}(M_{Ai}^2 + M_{Bi}^2 + M_{Ci}^2) \tag{4}$$

where n is total number of experiments, h is denotes number of factors, M_{Ai} is total observation of level i in factor A. Such as total observation of tooth thickness as shown in Table 4, M_{Ai} =359+245+236=840.

Thus, statistics of three factors A, B and C were expressed by F_A, F_B, and F_C respectively, which is determined using Eqs. (5)-(7).

$$F_A = \frac{KS_A}{S_e} \tag{5}$$

$$F_B = \frac{KS_B}{S_e} \tag{6}$$

$$F_c = \frac{KS_c}{S_e} \tag{7}$$

where $K = \frac{n-3h+2}{h-1}$

3.4. Analysis of Variance

Table 5 shows the variance analysis of each factor on index root stress. The F test can be used to determine the confidence range of each factor affecting the index, to analyze the influence of each factor. By comparing results of variance sum of various factors, influence order of various factors is determined preliminarily [24-25].

Table 5

Variance analysis of each factor on tooth root stress

Factor	Square of deviance	Freedom	Mean square	F	Confidence range
A	673	2	336	3.57	*
B	13082	2	6541	69.58	***
C	2867	2	1433	15.24	**
Error sum of squares	188	2	94	--	--
Sum	16810	8	--	--	--

where: Factors A, B and C are tooth thickness, tooth height and tooth root thickness, respectively. F is F test. *, * * and * * * are confidence levels below 90 %, 90 % - 95 % and above 95 %, respectively. -- is blank[9].

According to the analysis of variance of tooth root stress in table 5, the confidence level of factor B is above 95 %, which has obvious influence. The confidence of factor C is 90 % - 95 %, which has a relatively significant influence. the confidence of factor A was less than 90 %, and there was no significant effect. By comparing the square sum of the deviation of each factor, the order of influence on the stress on the sprocket tooth is B > C > A.

The order of influence of variance is consistent with the results of the analysis of range. In design and manufacture of a sprocket, due to the limitation of actual conditions, it may be impossible to change the three parameters at the same time to improve the sprocket strength. So, one or two size parameters of the sprocket can be changed to improve its bearing strength based on the influence of various factors.

4. Results Comparison

Under the same boundary conditions and friction parameters, the rigid-flexible coupling simulation of optimized sprocket is carried out. And then based on the rigid-flexible coupling simulation results, the fatigue life of a tooth of the sprocket is calculated by using the dynamic stress recovery method. And stress and fatigue nephogram of the sprocket under different working conditions are obtained as shown in Figure 7.

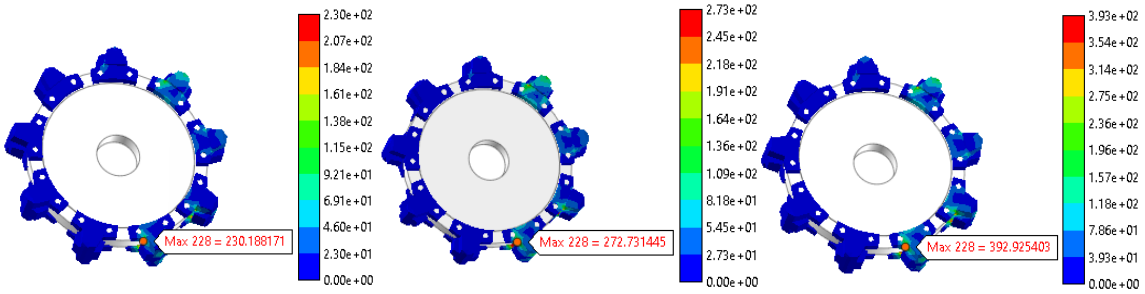

i) Straight road conditions ii) Hill climbing conditions iii) In-situ steering conditions

a) Sprocket teeth stress nephogram (MPa)

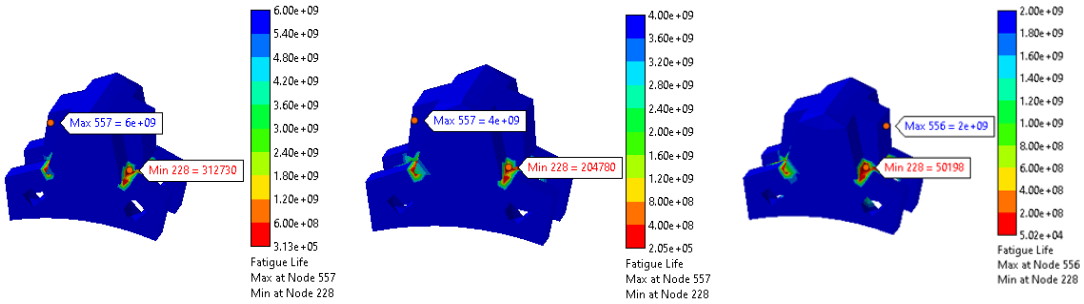

i) Straight road conditions ii) Hill climbing conditions iii) In-situ steering conditions

b) Sprocket teeth fatigue nephogram

Fig.7. Stress and fatigue nephogram of optimized sprocket teeth

It can be seen from Figure 7 that the maximum stress of the optimized sprocket tooth is reduced and its fatigue life is improved under typical working conditions, and its minimum fatigue life is more concentrated in the root of sprocket teeth. Therefore, only the root area of the sprocket tooth can be modified in the design and manufacture of the sprocket, to improve service life of whole sprocket tooth.

Compared with simulation results of optimized front sprocket tooth, the root stress of Optimized sprocket tooth is improved. The maximum stress of tooth root is decreased respectively by 10.1 %, 13.8 %, 7.5 %, and its fatigue life is increased respectively by 12.9 %, 17.1 %, 8.9 % under three working conditions of straight road, hill climbing, and in-situ steering. Under actual working conditions, crawler travel mechanism of a spreader will experience three typical working conditions, and the maximum stress of sprocket tooth is the largest and the fatigue life is the smallest under in-situ steering condition. Therefore, the stress of sprocket tooth is reduced by 7.5 %, and the fatigue life is increased by 8.9 %, which effectively improves service life of sprocket tooth and increases its reliability.

5. Conclusion

This paper use rigid-flexible coupling method to analyze sprocket strength of a spreader. The key dimensions of sprocket teeth are optimized based on orthogonal principle to improve service life of driving wheel. The following conclusions are drawn:

(1) The model of crawler walking mechanism is simulated and the driving torque of driving wheel is obtained. The simulation value of driving torque is compared with the theoretical value, and the error is less than 10 %, which verifies the correctness of the model.

(2) The results of orthogonal test are analyzed by variance and range method. The significance order of three factors obtained by the two methods on the stress of the tooth root is the same, and the order are B > C > A. The optimal size combination of sprocket teeth was obtained as factor A 166 mm, factor B 136 mm, and factor C 60 mm.

(3) After optimization of sprocket tooth, the results of rigid-flexible coupling simulation under typical working conditions showed that the maximum stress of tooth root is reduced by 7.5 % and its fatigue life is increased by 8.9 % under different working conditions, improving fatigue life of sprocket teeth.

Acknowledgements

The authors would like to thank the Key Research and Development Progr am of Shanxi Province (Grant No.202102010101010) for their support.

R E F E R E N C E S

[1]. *D. Guolong, Q. Yuan, M. Tingbo, Z. Daxing and Y. Yunqing*, "Modification method of cycloidal gears based on contact stress equalization", China Mechanical Engineering, **vol. 30, no. 9**, 2019, pp. 1081-1089. (in Chinese)

[2]. *C. Wang*, "Multi-objective optimal design of modification for helical gear", Mechanical Systems and Signal Processing, **vol. 157,** 2021, pp. 107762.

[3]. *Z. Y. Ren, S. M. Mao, W. C. Guo and Z. Guo*, "Tooth modification and dynamic performance of the cycloidal drive", Mechanical Systems and Signal Processing, **vol. 85**, 2017, pp. 857-866.

[4]. *P. F. Yan, H. Liu, P. Gao, X. Zhang, Z. B. Zhan and C. Zhang*, "Optimization of distributed axial dynamic modification based on the dynamic characteristics of a helical gear pair and a test verification", Mechanism and Machine Theory, **vol. 163**, 2021, pp. 104371.

[5]. *C. Wang, S. R. Wang and G. Q. Wang*, "A calculation method of tooth profile modification for tooth contact analysis technology", Journal of the Brazilian Society of Mechanical Sciences and Engineering, **vol. 40**, **no.7**, 2018, pp. 1-9.

[6]. *W. Yin, G. Zhou, D. Liu, Q. Meng, Q. Zhang and T. Jiang*, "Numerical simulation and application of entrainment dust collector for fully mechanized mining support based on orthogonal test method", Powder Technology, **vol. 380**,2021, pp. 553-566.

[7]. *K. Yuchun, C. Yonglong and M. Taoyuan*. "Performance analysis and structural parameter optimization of high bending drilling tool joints for slim hole window sidetracking", China mechanical engineering, **vol. 30, no. 24**, 2019, pp. 3010-3017. (in Chinese)

[8]. *L. Guimin, Y. Zhongxu, Z. Yifan, Y. Tao and W. Min*, "Research on micro-structure and properties of supersonic plasma sprayed Mo coatingbased on orthogonal experiment", Acta armamentarii, **vol. 37, no. 8**, 2016, pp.1489-1496. (in Chinese)

[9]. *S. Tang, S. Yuan, J. Hu, X. Li, J. Zhou and J. Guo*, "Modeling of steady-state performance of skid-steering for high-speed tracked vehicles", Journal of Terramechanics, **vol. 73**, 2017, pp. 25-35.

[10]. *S. Y. Chen, L. M. Wang and W. Shi*, "Application of virtual substance in launch dynamics simulation for self-propelled guns", Applied Mechanics and Materials, **vol. 236** 2012, pp. 1296-1301.

[11]. *N. V. Namboothiri and P. Marimuthu*, "Investigation of fracture behavior of asymmetric spur gear", Theoretical and Applied Fracture Mechanics, **vol. 114**, 2021, pp. 102991.

[12]. *O. Doan, C. Yuce and F. Karpat*, "Effects of rim thickness and drive side pressure angle on gear tooth root stress and fatigue crack propagation life", Engineering Failure Analysis, **vol. 112**, 2021, pp. 105260.

[13]. *M. L. Puneeth and G. Mallesh*, "Dynamic contact behavior of asymmetric spur gear", Materials Today: Proceedings, **vol. 44**, 2021, pp. 2019-2027.

[14]. *S. Chavadaki, K. Kumar and M. N. Rajesh*, "Finite element analysis of spur gear to find out the optimum root radius", Materials Today: Proceedings, **vol. 46**, 2021, pp. 10672-10675.

[15]. *H. Mao, Y. Zhang, H. Mao, Z. Huang, J. Fan, X. Li and X. Li*, "The fatigue damage evaluation of gear in sugarcane presser using higher order ultrasonic nonlinear coefficients", Results in Physics, **vol. 10**, 2018, pp. 601-606.

[16]. *I. I. Berezin and A. A. Abyzov*, "Probabilistic modeling of tracked vehicle mover and ground interaction", Procedia Engineering, **vol. 206**, 2017, pp. 432-436.

[17]. *H. He, H. Liu, C. Zhu, P. Wei and Z. Sun*, "Study of rolling contact fatigue behavior of a wind turbine gear based on damage-coupled elastic-plastic model", International Journal of Mechanical Sciences, **vol.141**, 2018, pp. 512-519.

[18]. *S. Li and A. Anisetti*, "A tribo-dynamic contact fatigue model for spur gear pairs", International Journal of Fatigue, **vol.98**, 2017, pp. 81-91.

[19]. *K. H. Lee, J. W. Yi, J. S. Park and G.J. Park*, "An optimization algorithm using orthogonal arrays in discrete design space for structures", Finite Elements in Analysis and Design, **vol. 40**, **no.1**, 2003, pp.121-135.

[20]. *A. S. Hedayat, J. Stufken and G. Su*, "On difference schemes and orthogonal arrays of strength t", Journal of statistical planning and inference, **vol. 56**, **no.2**,1996, pp.307-324.

[21]. *C. X. Ma, K. T. Fang and E. Liski*, "A new approach in constructing orthogonal and nearly orthogonal arrays", Metrika, **vol. 50**, **no.3**, 2000, pp. 255-268.

[22]. *V. Ayhan and S. Tunca*, "Experimental investigation on using emulsified fuels with different biofuel additives in a DI diesel engine for performance and emissions", Applied Thermal Engineering, **vol.129**, 2018, pp. 841-854.

[23]. *D. Y. Jiang*, "Study on parameter optimization for cutting safety and efficiency of premixed abrasive water jet for htpb propellant", U.P.B. Sci. Bull., Series D, **Vol. 83**, **no.1**, 2021, pp. 205-220.

[24]. *J. Yu, Y. Qin, P. Gao, Y. Han and Y. Li*, "An innovative approach for determining the grinding media system of ball mill based on grinding kinetics and linear superposition principle", Powder Technology, **vol.378**, 2021, pp. 172-181.

[25]. *J. S. Liu, C.Q. Gao, Y. J. Nie, B. Yang, and Z. H. Xu*, "Numerical simulation of Fertilizer Shunt-Plate with uniformity based on EDEM software", Computers and Electronics in Agriculture, **vol.178** 2020, pp. 105737.